

Final Technical Report

NCC 2-5377

**DEVELOPMENT AND APPLICATION OF NOVEL  
DIAGNOSTICS FOR ARC-JET CHARACTERIZATION**

**NASA-Ames University Consortium**

**Prepared for**

**Dr. George Raiche, Collaborator at the NASA-Ames Research Center**

**For the Period**

**April 1, 2000 to September 30, 2002**

**December 2002**

**Submitted by**

**R. K. Hanson, Principal Investigator**

**HIGH TEMPERATURE GASDYNAMICS LABORATORY  
Mechanical Engineering Department  
Stanford University**

CASI

**"Development and Application of Novel Diagnostics  
for Arc-Jet Characterization"**

April 1, 2000 to September 30, 2002

## **1. Introduction**

The development of new sensors to characterize the energy partitioning in the plume of the NASA Ames arcjet plume is described. This arcjet is an important facility in the testing of thermal protection material. These materials are crucial to the survival of planetary and inter-planetary space vehicles. Without thermal protection, these vehicles would be destroyed as they re-enter the earth's (or target planet's) atmosphere. The NASA Ames arcjet plume simulates these harsh re-entry environments and can test spacecraft thermal management materials.<sup>1-6</sup> However, the energy balance used to predict test environment conditions for these thermal management materials remains a research problem. A high enthalpy supersonic gas flow is produced by expanding arc-heated gas through a converging-diverging nozzle. Accurate assessment of the material test conditions requires understanding of the flow properties. Even though, the arcjet facilities have been used for several decades, the extremely harsh environment inhibits complete flow characterization. Especially troublesome are the impurities in the flow from electrode erosion and the amount of energy sequestered into metastable electronic energy levels of molecular nitrogen, atomic argon, and atomic oxygen.

In this report, development of a sensor suite based on tunable diode laser absorption spectroscopy is described. These sensors will monitor the chemical composition of the plume to quantify the concentration of impurities from electrode erosion in the arc-heater and in the test cell monitor species in metastable electronic excited states in the plasma plume. The sensor strategies are based on diode laser absorption and exploit the expertise developed previously at Stanford University. Baer<sup>7-10</sup> investigated the temperature and the number density of atomic Ar in its metastable excited electronic state ( $^3P_{0,2}$ ) in atmospheric pressure plasmas, using a scanned wavelength direct absorption strategy over spectrally resolved transitions near 811.5, and 810.4nm. Chang and Baer<sup>11</sup> also measured electronically excited atomic oxygen by scanning two transitions near 777.2nm in atmospheric-pressure, argon/oxygen plasma. Recently, the Ar transition near 811.5nm was employed to monitor electronically excited Ar in an arcjet plume.<sup>12-13</sup>

## **2. The Energy Partition Problem in the Arcjet Plume**

The major species in high temperature (4000-10000K) air are molecular and atomic nitrogen, molecular and atomic oxygen, nitric oxide, and nitric-oxide ions.<sup>14-15</sup> In addition to air, the arcjet feedstock contains a significant fraction of argon. At the very high temperatures in the arc-heater and plume, there can be significant population in excited electronic states. Resonance transitions of these species lie in the vacuum ultra violet where quantitative emission techniques are difficult. In addition, there can also be

a significant fraction of the population in the metastable excited electronic manifolds of these species. When the arc-heated gas expands into the arcjet plume, the excited resonance states can radiatively relax. However, excited species in their metastable manifolds only radiatively relax to the lowest electronic metastable state. The arcjet expansion can isolate these species from collisional deactivation, and some of these excited species can be trapped in their lowest metastable electronic level for times longer than the transit time between arcjet expansion and the test model. Each of these electronic excited states has energy of several eV, and thus significant energy can be sequestered in these excited species. The concentration of such species must be understood to properly model the arcjet gas energy distribution. The long radiative lifetime of these metastable species precludes their measurement by emission techniques. In this work, we target metastable state concentrations in the arcjet plume and concentrations of impurities in the arc-heater.

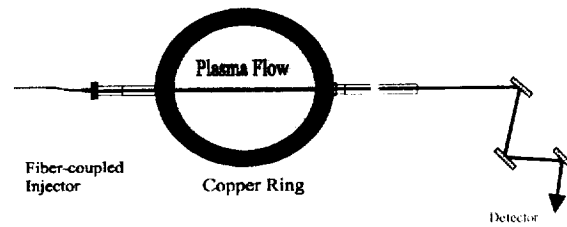
### **3. Project Goals and Accomplishments**

This NASA-Ames University Consortium Project: "Development and Application of Novel Diagnostics for Arc-Jet Characterization" has focused on the design and demonstration of optical absorption sensors using tunable diode laser to target atomic copper impurities from electrode erosion in the arc-heater metastable electronic excited states of molecular nitrogen, atomic argon, and atomic oxygen in the arcjet plume. Accomplishments during this project include:

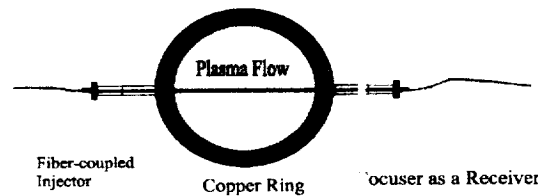
1. Design, construction, and assembly of optical access to the arc-heater gas flow.
2. Design of diode laser sensor for copper impurities in the arc-heater flow.
3. Diode laser sensor design and test in laboratory plasmas for metastable  $\text{Ar}(^3\text{P})$ ,  $\text{O}(^5\text{S})$ ,  $\text{N}(^4\text{P})$ , and  $\text{N}_2(\text{A})$ .
4. Diode laser sensor demonstration measurements in the test cell to monitor species in the arcjet plume.

### **4. Sensor Design for Atomic Copper**

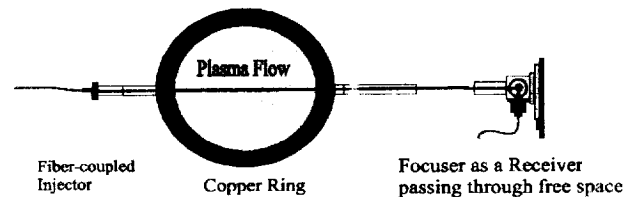
We developed a strategy to detect atomic copper in the arc-heated, high temperature, high density pre-expansion region. We have refined our initial scheme to incorporate fiber-coupled sensors to produce a safe, robust sensor system. The design is depicted in Fig.1 (a): the laser beam passes through the copper ring across the plasma flow and is recollected through the copper ring. In this first design the transmitted light is propagated in free space with mirrors to the detector. However, tests at NASA show that the vibration induces beam steering that seriously degrades the signal collection. A fiber-coupled transmitter/receiver system was subsequently designed. The foremost engineering problems for this fiber-coupled scheme is collection of the beam after it passes through the plasma flow and coupling this beam into the detector fiber as depicted in Fig.1 (b).



(a) mirror scheme



(b) fiber-coupled scheme



(c) fiber-coupled scheme

Fig.1. Three detection schemes for the copper sensor. (a) is original mirror scheme and (b), and (c) are the improved schemes using optical fiber-coupled detection strategies.

Free space propagation of the beam to the wall of the safety enclosure and subsequent coupling to a fiber was also considered as shown in Fig 1(c). The additional free space path length reduces the f/number of the optical collection and thus reduces the interference from plasma emission. These new designs are complete and ready for test.

## 5. Design and Test of Plume Sensors

The project goal is the development of a user friendly sensor based optical absorption of a wavelength scanned diode laser. Thus, the potential transitions are limited to those which overlap the optical region where diode lasers are readily available: the near infra-red (NIR) between 1260 and 1660 nm and the visible and far-red region between 640 and 900 nm. Atomic transition data is readily available.<sup>16-20</sup> The spectroscopy of the Ar, N, O, and N<sub>2</sub> was examined, and transitions to probe the concentration of the lowest metastable electronic excited states were explored. Fortunately each of these major species has absorption transitions from their metastable excited electronic states which overlap with available diode lasers. Using the NIST database candidate absorption transitions were selected and tabulated.

Spectra simulation of air by Laux at 7000K and at 1atm is shown in Fig. 2. This condition is similar to the condition at the nozzle throat (actual pressure at the throat is approximately 2 atm; however, and the simulation was limited to 1 atm). At this high

temperature the equilibrium mole fraction of each species is pressure dependent. Using the detailed chemistry code, Chemkin, we find the maximum mole fraction variation is less than 30% when the pressure is doubled at this temperature. Thus we can estimate the wavelength integrated absorbance is simply proportional to pressure with a  $\pm 30\%$  uncertainty.

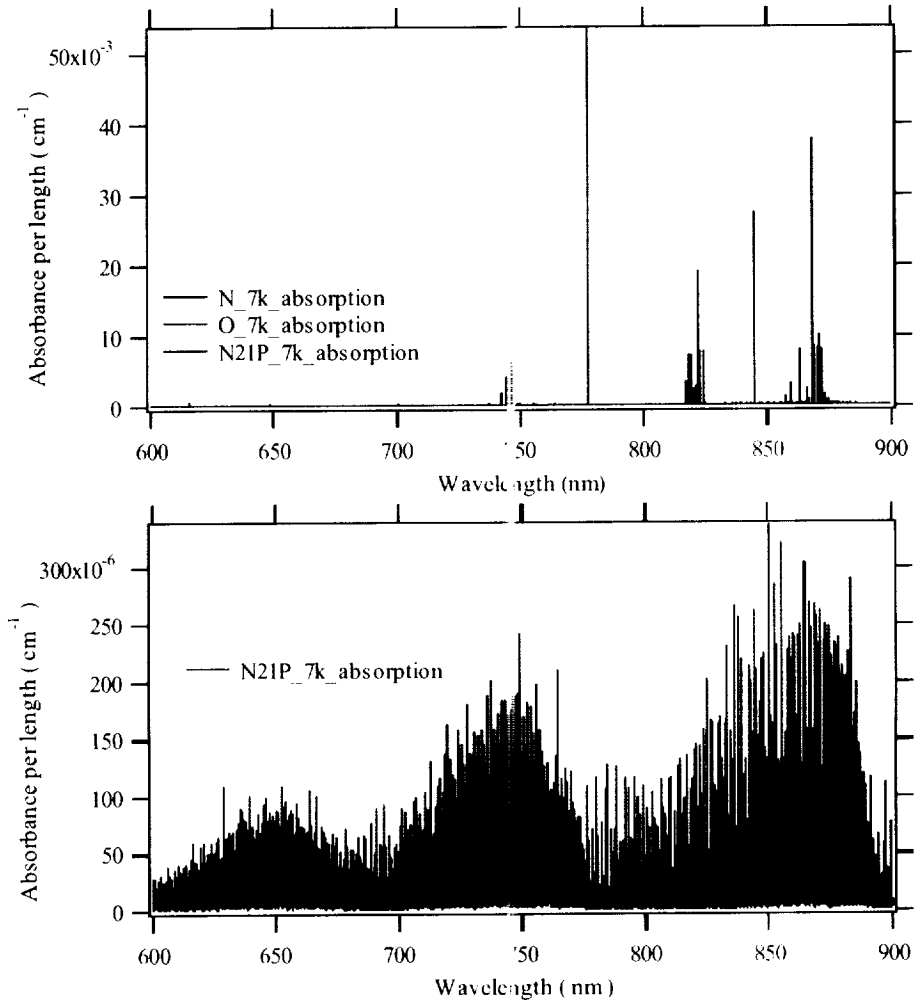


Fig. 2. Simulated absorbance by the nitrogen and oxygen components of the arcjet plume at 7000K; lower panel shows the detail of the absorbance of the molecular nitrogen first positive.

Strong absorption for atomic oxygen near 777nm ( $^5S$ ) and 844nm ( $^3S$ ) is expected. In addition we see atomic nitrogen absorption features near 746nm ( $^2P$ ), 824nm ( $^4D$ ), and 868nm ( $^4D$ ). The molecular  $N_2$  absorption in the first positive system ( $A^3\Sigma_u-B^3\Pi_g$ ) is about 100 times smaller in the region near 771nm. The lower panel shows the rich ro-vibrational absorption spectrum for the high temperature  $N_2$  ( $A^3\Sigma_u-B^3\Pi_g$ ). The target species,  $Ar(^3P)$ ,  $O(^5S)$ ,  $N(^4P)$ , and  $N_2(A)$ , are all electronic excited species which are metastable to allowed single photon transitions to the ground electronic state.

Before searching in the harsh environment of the arcjet plume we first investigated our diode laser sensor strategies in a microwave discharge flow reactor depicted in Fig. 3. An Evenson cavity surrounds a pyrex tube and is powered with a 1kW microwave generator (Ophos Instruments) at 2450 MHz. A slow, 10-30 sccm, flow (Tylan) of target gas (Ar, O<sub>2</sub>, or N<sub>2</sub>) is pumped through the reactor at a pressure between 0.5 and 2m Torr. The laser is directed through the discharge and focused onto a silicon photodiode. The laser is wavelength tuned by varying the diode injection current and the relative wavelength change was measured with a 2 GHz solid etalon.

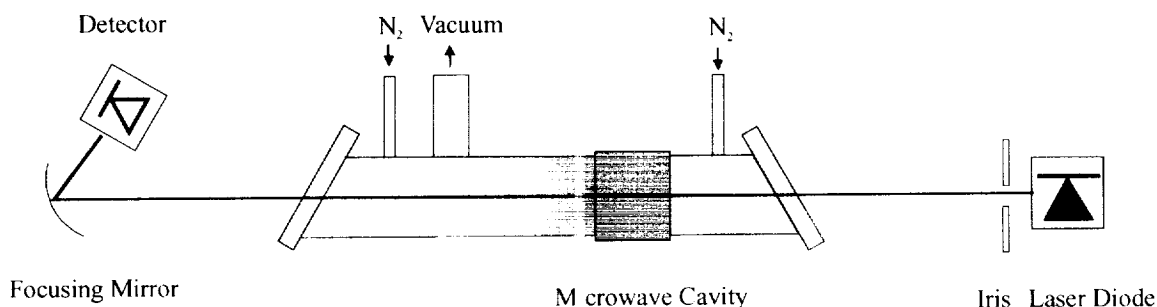


Fig. 3. Schematics of a discharge tube at Stanford University

## 5.1 Argon

A portion of the argon energy levels and transitions are presented in Fig. 4, which terminate on the ( $4s^3P$ ). Two of the  $4s^3P$  states are metastable to allowed single photon transitions to the ground state ( $4s^3P_{0,2}$ ). The three transitions near 810, 811, and 842 nm were used by Baer and Hanson<sup>7</sup> to detect metastable argon atoms in a inductively heated plasma. In this work, we initially select the two transitions near 772 nm (772.38, and 772.42 nm) to exploit the possibility of measuring the population of two different lower states by wavelength tuning a single diode laser.

The electronically excited atomic argon was observed in the Stanford University discharge flow reactor in a 25W argon plasma at a pressure of 0.4 Torr. Fig. 5 shows the absorption feature from the  $4s^1 2J=1$  transition near 772 nm. The laser wavelength was scanned across the transition at 500 Hz and a 25 scan average (50ms) gave a minimum detectable absorbance of  $4 \times 10^{-4}$  ( $5 \times 10^6 \text{ cm}^{-3}$ ) for direct absorption of the wavelength scanned laser. The width of the absorption line at this low pressure is dominated by Doppler broadening and the kinetic (translational) temperature is inferred to be approximately 700K. A similar measurement on the  $4s^3 2J=1$ , provided a number density of  $2.7 \times 10^8 \text{ cm}^{-3}$  in this discharge.

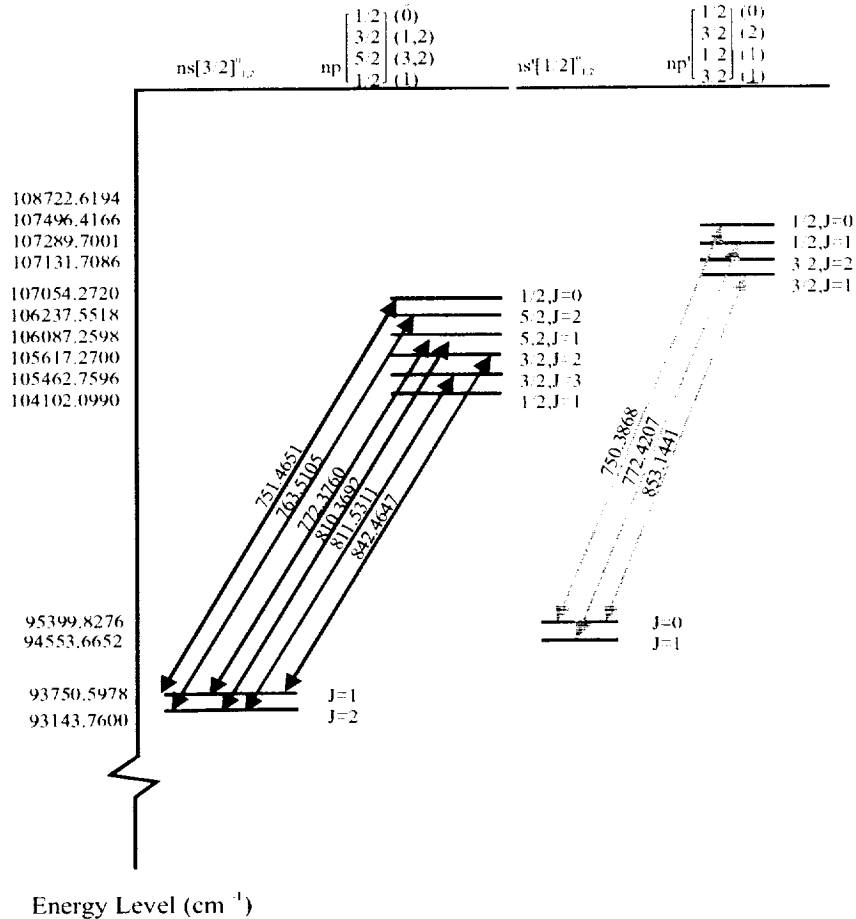


Fig. 4 Partial energy level diagram for argon

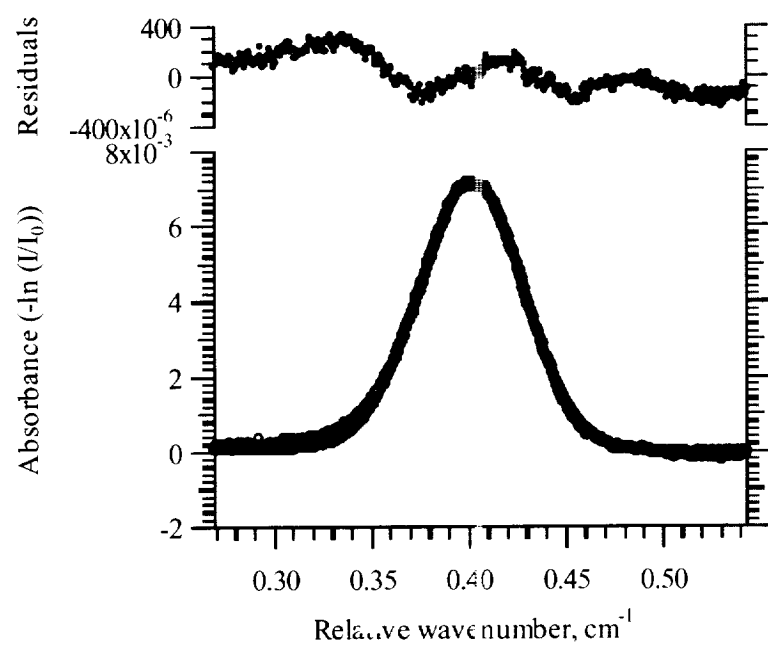


Fig. 5 Atomic argon absorption lineshape at 772nm



## 5.2 Atomic Oxygen

Fig. 6 shows a portion of the energy levels and transitions for atomic oxygen. Previous work in a discharge flow combined actinometry with VUV absorption technique.<sup>21-23</sup> Transitions which overlap with available diode lasers include those near 645, 777, and 844 nm. Detection of the metastable  $^5S$  state with absorption near 777 nm is chosen for our measurements because these three transitions are sufficiently close to be accessible with a single diode laser.

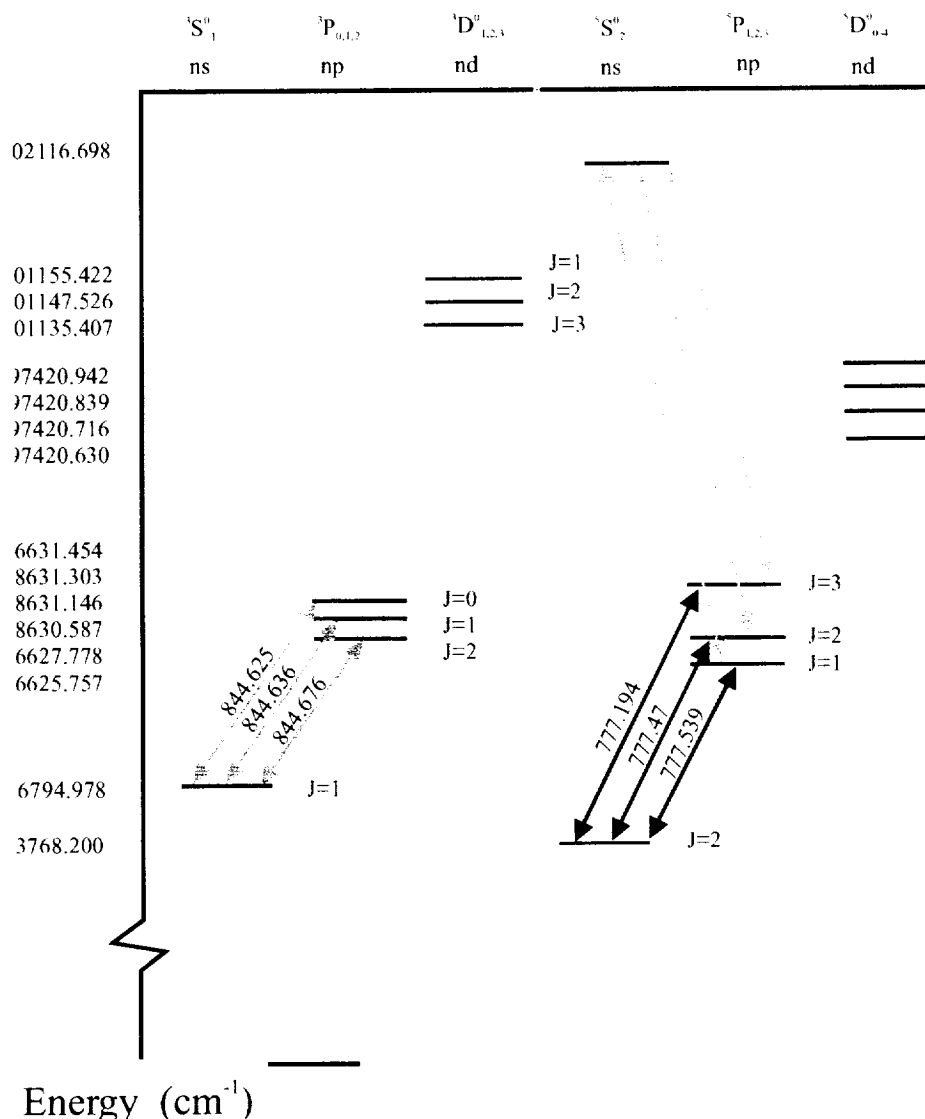


Fig. 6. Partial energy level diagram for atomic oxygen

Detection of  $^5S$  atomic oxygen was demonstrated in Stanford discharge flow reactor. Fig. 7 shows an absorption lineshape taken in a 25W plasma in a slow (13 sccm) of oxygen at 0.39 Torr. This scan shows an 8% absorbance was observed at the line center corresponding to a number density in the  $^5S^0_2$  of  $6.0 \times 10^7 \text{ cm}^{-3}$ . Using a 25 scan

average (50ms) the minimum detectable absorbance was approximately  $1 \times 10^{-3}$  for direct absorption. From the lineshape the kinetic (translational) temperature was estimated at 900 K. At this temperature the detection limit is  $1 \times 10^6 \text{ cm}^3$ . Although all three transitions were monitored, here only the 777.2nm transition ( $^5S_2^0 \rightarrow ^5P_3$ ) is shown.

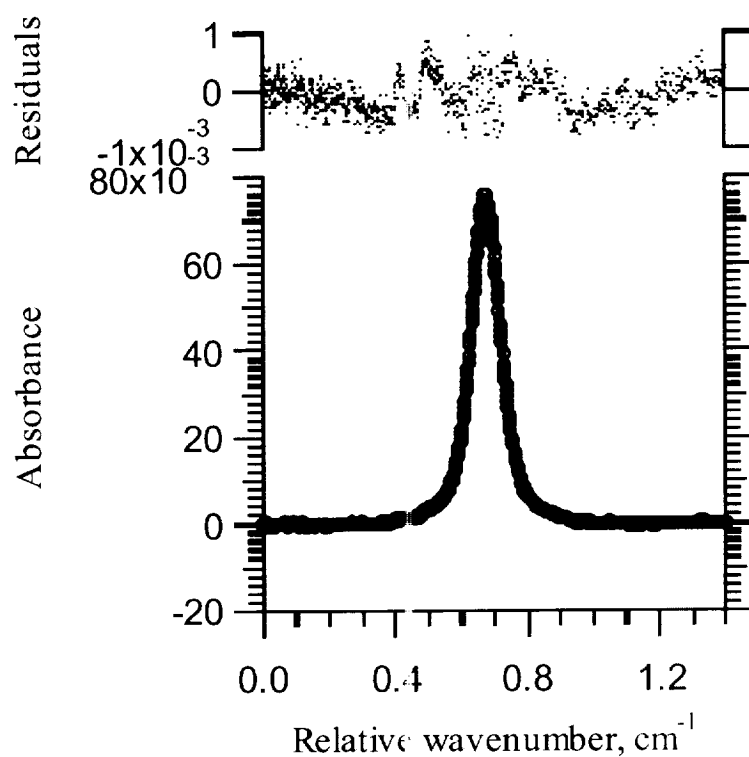
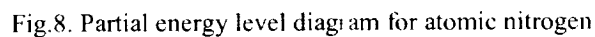


Fig. 7 Atomic oxygen absorption lineshape at 777nm

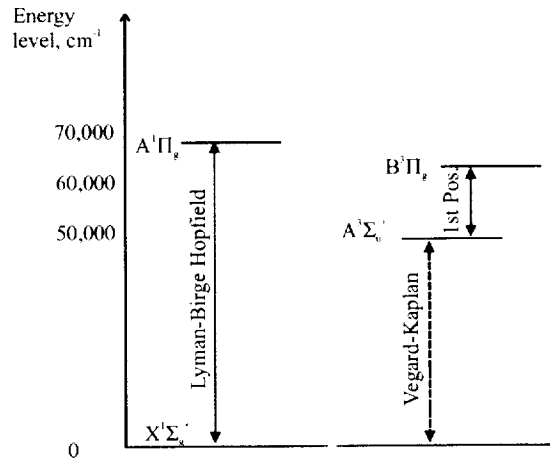
Fig. 8 shows a portion of the energy levels and transitions for atomic nitrogen. The transition at 868.02 nm is the strongest absorption line based on simulations. The transitions around 740 nm can also be used to monitor the  $^4\text{P}$ .



#### 5.4 Molecular Nitrogen

At the throat of the arc-heated expansion, the temperature peaks at nearly 10,000K, and nitrogen molecules in the gas are primarily dissociated into nitrogen atoms. However, the cooling in the expansion induces recombination of atomic nitrogen. The intense radiation indicates that a large fraction of the recombined nitrogen is electronically excited. Singlet and triplet manifolds of excited states quickly radiate to their lowest electronic state. For the singlet molecules this is the  $X^1\Sigma_g^+$  ground state and for the triplet molecules this is the meta-stable  $A^3\Sigma_u^+$ . The relevant energy levels are illustrated in Fig. 9. This lowest-lying triplet electronic state is radiatively coupled to the ground state via the triplet to singlet forbidden Vegard-Kaplan bands. Their radiative lifetime is too long to deplete this energy storage until long after the expansion flow has interacted with the test model. However, these triplet molecules can also be relaxed early in the flow by collisions before the free stream of the expansion is developed. Therefore, it is important to investigate and quantify this potential energy storage to develop more accurate codes for arc-jet flow simulation.  $N_2$  first positive band has been studied for a few decades.<sup>6,24-29</sup>

a)



b)

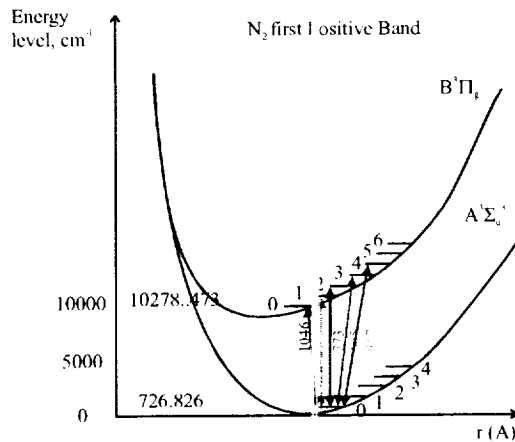


Fig. 9 (a) Energy level spacing for selected electronic transitions in molecular nitrogen, (b) detail for the metastable first positive system

The spectroscopic parameters are known well enough to predict the line positions and shapes; with assistance from C. Laux, we simulated a spectrum for typical test conditions, shown in Fig. 10. The fraction of excited  $N_2(A)$  is assumed to be equilibrium and does not include the potential for energy pooling in the metastable state as studied by G.Callede.<sup>30</sup>

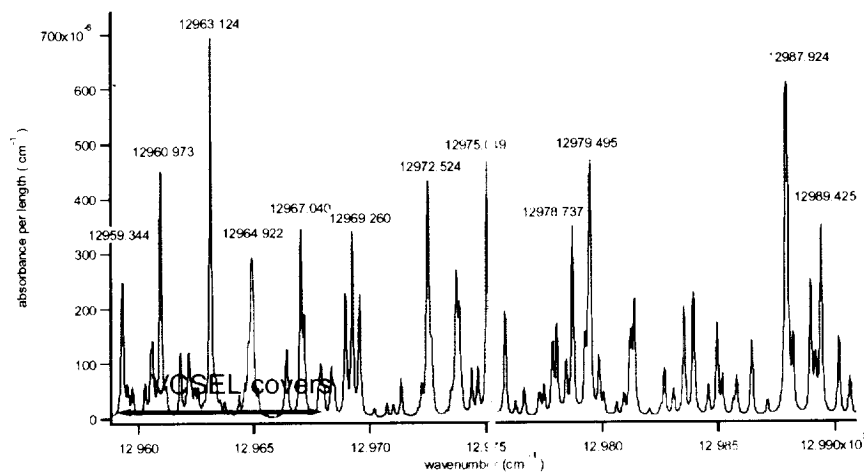


Fig. 10. Simulated  $N_2$  first positive band spectra, assuming an electronic temperature of 5000K, vibrational temperature of 2000K, rotational and translational temperature of 800K at 1atm

Other work in our laboratory and elsewhere have demonstrated that the device architecture of a vertical cavity surface emitting laser, VCSEL, is capable of a rapid wavelength scanning of a broad spectral range compared to DFB diode lasers.<sup>31-32</sup> The VCSEL source has low intensity noise; e.g. using a balanced detection technique, shot noise limited detection of oxygen was demonstrated.<sup>33</sup> Figure 10 shows a VCSEL scan of more than  $10\text{ cm}^{-1}$  near 771 nm; thus, wavelength scanning over multiple few transitions is possible. Standard DFB diode laser architecture typically restricts the scan range to 1 or  $2\text{ cm}^{-1}$ . The transition  $v''=0 \rightarrow v'=2$  of the  $1^1_1$  positive band is near 773nm and can be detected at 771.4nm or  $12963\text{ cm}^{-1}$  with VCSEL light absorption.

In the Stanford discharge flow reactor, we observed 0.15% maximum absorbance for nitrogen the first positive system at the pressure of 0.5Torr and input power of 20W in nitrogen gas with a flow rate of 20 sccm. The absorbance shown in Fig. 11 is fitted to Doppler lineshape, and its area gave the number density of  $A\ \Sigma_u^+ (v'=0, J=13)$ . Data was averaged for 50ms and the detection limit of  $2 \times 10^{-4}$  was achieved with direct absorption methods. The kinetic (translational) temperature, was measured at 1200 ~ 1400 K and the number density  $3.0\text{-}4.0 \times 10^{10}\text{ cm}^{-3}$ . We find a direct absorption detection limit of  $1 \times 10^9\text{ cm}^{-3}$  in this low-pressure plasma.

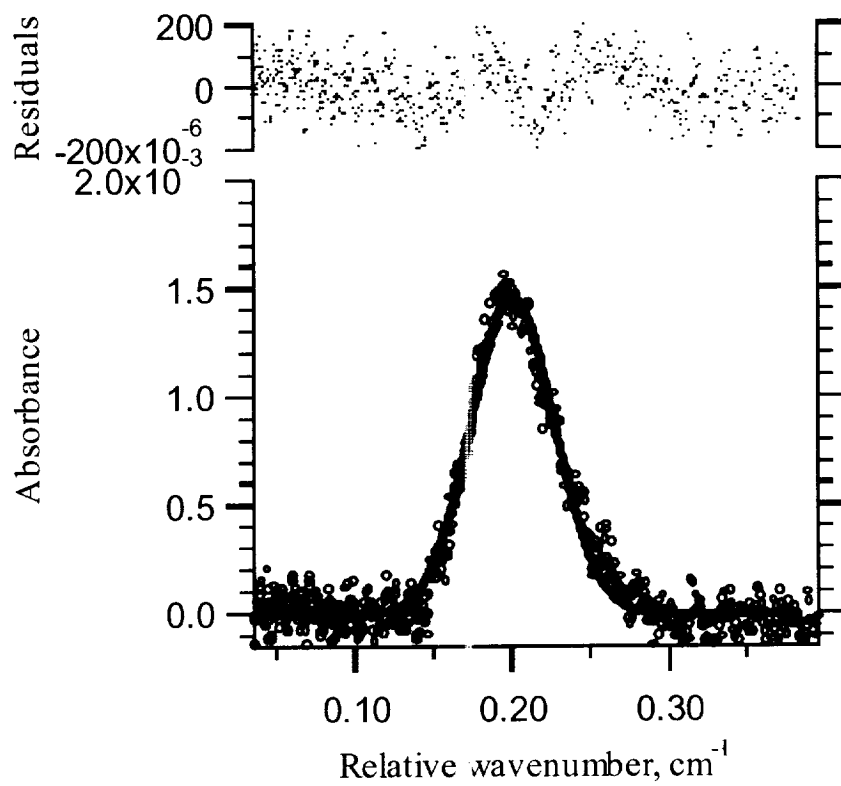


Fig. 11 Transition at 773nm N<sub>2</sub> first positive system.

## 6. Diode Laser Sensors in the Arcjet Facility at NASA Ames

In addition to testing our diode laser sensor strategies in the discharge tube at Stanford University, we also installed and began initial testing of the sensors in the arcjet facility at NASA Ames Research Center. The light from the diode lasers is multiplexed and coupled into a fiber for delivery into the electrically isolated test cell. The electrical isolation of the test cell is a firm safety requirement and the fiber coupled laser optics solves this experimental issue. Once the light is in the test cell, a fiber collimator (injector) pitches the laser beams across the post expansion plasma plume, the beam is then retro-reflected to double the path length and simplify the installation of return optical fibers, and the light is re-coupled into a receiver fiber to exit the test cell for remote detection. The retro-reflection mirror has a focal length of 2 m to mitigate beam dispersion.

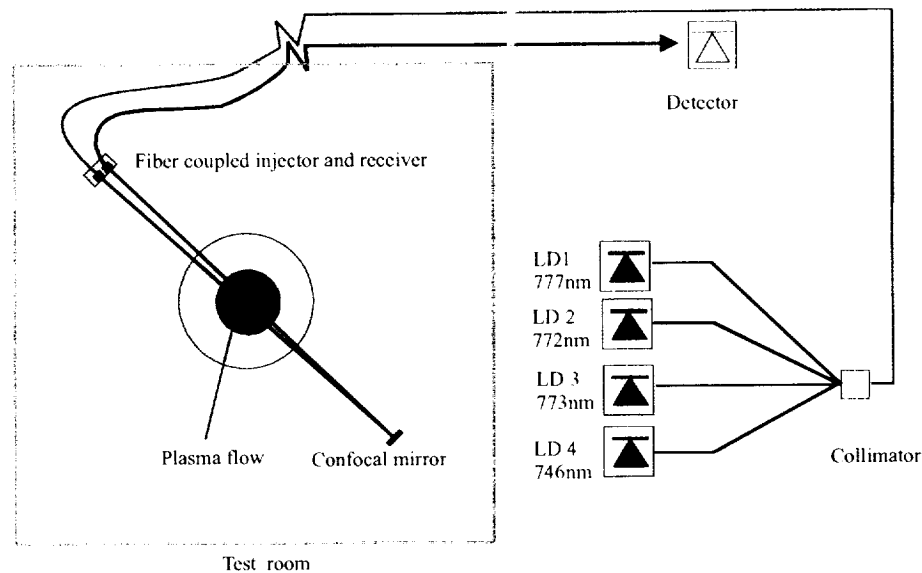


Fig. 12 Schematics of diode laser sensors in the arcjet test cell:  
fiber-coupled laser transmission is designed to ease the alignments and to isolate the test cell

There are two important interference problems: first, the bright optical emission from the plasma produces background light and second, the radiative emission of the plasma and thermal emission from plasma heated model is sufficiently intense to heat the optical components causing damage and misalignment. The small f-number of the low numerical aperture fiber essentially eliminates plasma emission interference at the cost of stringent optical alignment requirements. Unfortunately, the small f-number also makes the optical collection more sensitive to thermal misalignment. The remainder of the sensor set-up is rather standard. However, note that the low resistance of vertical cavity surface emitting diode lasers (VCSELs) requires a ultra-low noise function generator for accurate and reproducible wavelength tuning. Temperature and injection current

controllers are used to fix the center wavelength of laser outputs at the desired wavelength respectively.

The arcjet test sequence is as follows: (1) air in the test chamber is pumped down at low pressure ( $\sim$  Torr) (2) the discharge is started on pure argon (3) air is mixed with argon (4) test model or material is moved into the center of plasma plume (5) discharge is turned off (6) the pressure in the test chamber is restored up to 1atm (7) test model or specimen is removed from the test room.

Initial experiments successfully monitored excited argon atoms in the initial start-up phase as shown in Fig. 13. Thermal misalignment of the fiber collection optics foiled experiments in the air plasma. A new design should mitigate the radiative heating by mounting the optical components on the ceiling and the sidewall and providing more substantial radiation shields. The new mounting positions significantly reduce the solid angle for the radiative heating. In addition, cold nitrogen gas will be used to purging and cool the optical components.

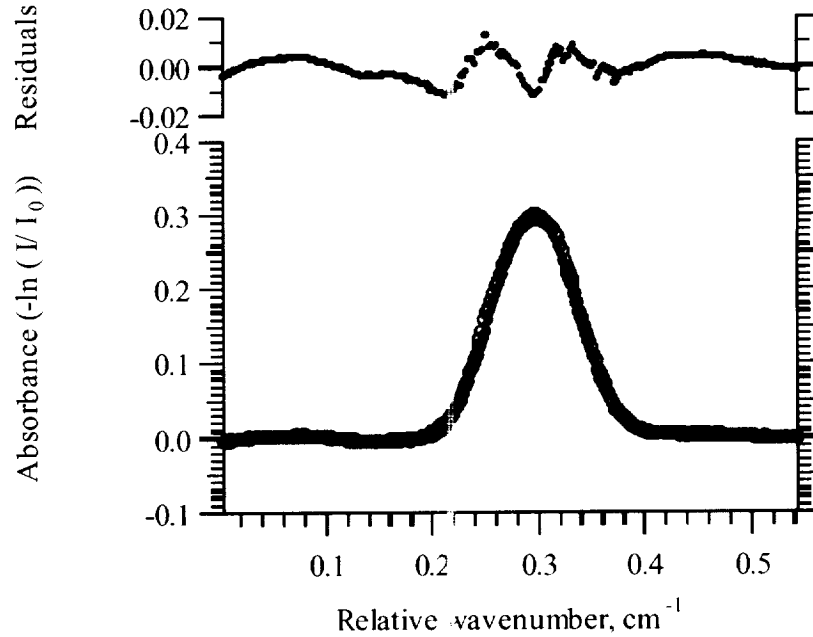


Fig. 13 Direct absorption near 772.38nm monitoring excited argon atoms from  $3s3/2 J=1 \rightarrow 4p5/2 J=1$



References:

1. C.Scott, "Survey of Measurements of Flow Properties in Arcjets," J. Thermophys. Heat Transfer **7**, 9-24 (1993)
2. D.Babikian, N. Gopaul, and C.Park, "Measurement and Analysis of Nitric Oxide Radiation in an Arcjet Flow," J. Thermophys. Heat Transfer **8** 737-743 (1994)
3. D.G.Fletcher, "Arcjet Flow properties Determined from Laser-Induced Fluorescence of Atomic Nitrogen", Applied Optics, 1999
4. C.S.Park, M.E.Newfield, D.G.Fletcher, T.Gokcen, and S.P.Sharma, "Spectroscopic Emission Measurements Within the Blunt-Body Shock Layer in an Arcjet Flow", Journal of Thermophysics and Heat Transfer, Vol.12, pp.190-197, 1998
5. D.J.Bamford, A.O'Keefe, D.S.Babikian, D.A.Stewart, and A.W.Strawa, "Characterization of Arcjet Flows Using Laser-Induced Fluorescence", Journal of Thermophysics and Heat Transfer, Vol.9, pp.26-33, 1995
6. M.Simek, G.Dilecce, and S.Benedictis, "On the use of the numerical simulation of the first positive system of N<sub>2</sub>: Emission and LIF analysis", Plasma Chemistry and Plasma Processing **15** 427-449
7. D.Baer, and R.Hanson, "Tunable Diode Laser Absorption Diagnostics for Atmospheric Pressure Plasmas", J.Quant.Spectrosc.Radiat.Transfer **47**, 455-475 (1992)
8. D.Baer, H.Chang, and R.Hanson, "Semiconductor-Laser Absorption Diagnostics of Atomic Oxygen in an Atmospheric Pressure Plasmas", J.Quant.Spectrosc.Radiat.Transfer **50**, 621-633 (1993)
9. D.Baer, H.Chang, and R.Hanson, "Fluorescence Diagnostics for Atmospheric-Pressure Plasmas Using Semiconductor Lasers", J.Opt.Soc.Am.B **9**, 1968-1978 (1992)
10. D.Baer, and R.Hanson, "Semiconductor Laser-based Measurements of Quench Rates in an Atmospheric Pressure Plasma by using Saturated-Fluorescence Spectroscopy", Appl.Opt. **32**, 948-955 (1993)
11. D.Baer, H.Chang, and R.Hanson, "Semiconductor-laser absorption diagnostics of atomic oxygen in an atmospheric-pressure plasma", J.Quant.Spectrosc.Radiat.Transfer **50** 621-633 (1993)
12. F.Zhang, K.Komurasaki, "Diagnostics of an argon arcjet plume with a diode laser", Appl.Opt. **38** 1814-1822 (1999)
13. F.Zhang, T.Fujiwara, and K.Komurasaki, "Diode-Laser tomography for arcjet plume reconstruction", Appl.Opt. **40** 957-964 (2001)
14. W.Vincenti, and C.Kruger, Introduction to physical gas dynamics, 1965, John Wiley & Sons, inc. New York
15. M.Mitchner, and C.Kruger, Partially ionized gases, 1973, John Wiley & Sons, inc. New York
16. [http://physics.nist.gov/cgi-bin/AtData/main\\_asd](http://physics.nist.gov/cgi-bin/AtData/main_asd)
17. <http://plasma-gate.weizmann.ac.il/DBfAPP.html>
18. <http://legacy.gsfc.nasa.gov/topbase/home.html>

19. A.Radzig, and B.Smirnov, Reference data on atoms, molecules, and ions, 1985, Spring-Verlag Berlin Heidelberg
20. G.Herzberg, Atomic spectra and atomic structure, 1945, Dover New York
21. A.Granier, D.Chereau, K.Henda, R.Safari, and P.Leprince, "Validity of actinometry to monitor oxygen atom concentration in microwave discharges created by surface wave in O<sub>2</sub>-N<sub>2</sub> mixtures", J.Appl.Phys. **75** 104-114 (1994)
22. A.Timofeev, "Theory of microwave discharges at atmospheric pressures", Plasma Physics Reports **23** 158-164 (1997)
23. A.Vikharev, A.Gorbachev, O.Ivanov, A.Kolysko, and O.Kuznestov, "Spatial structures of continuous microwave discharge", Journal of Experimental and Theoretical Physics **93** 324-378 (2001)
24. R.W.B.Pearse, and A.G.Gaydon, 1976, *The identification of molecular spectra*, Chapman and Hall.
25. L.G. Piper etc.1989, *Experimental determination of the Einstein coefficients for the N<sub>2</sub> (B-A) transition*, J.Chem.Phys. **90**, 5337-5345
26. S.D.Benedictis, G.Dilencece, and M.Simek, 1998, *LIF measurement of N<sub>2</sub> ( $A^3\Sigma_u^+$ , v=4) population density in a pulsed rf discharge*, J.Phys.D:Appl.Phys. **31** 1197-1205
27. P.R.Sasikumar, S.S.harilal, V.P.N.Nampoori, and C.F.G.Vallabhan, *High resolution optogalvanic spectrum of N<sub>2</sub>- rotational structure of (11,7) band in the first positive system*, Pramana J-phys., **42**, 231-237
28. F.Roux, and F.Michaud, 1990, *Investigation of the rovibrational levels of the B<sup>3</sup>Π<sub>g</sub> states of <sup>14</sup>N<sub>2</sub> molecule above the dissociation limit N(<sup>4</sup>S) + N(<sup>4</sup>S) by Fourier transform spectrometry*, Can.J.Phys., Vol.68,1257-1261
29. C.Laux, and C.H.Kruger, 1992, *Arrays of radiative transition probabilities for the N<sub>2</sub> first and second positive, NO beta and gamma, N<sub>2</sub>+ first negative, and O<sub>2</sub> Schumann-Runge band systems*, J.Quant.Spec.Radiat.Transfer Vol.48, 9-24
30. G.Callede, J.Deschamps, J.L.Godart, and A.Ricard, 1991, *Active nitrogen atoms in an atmospheric pressure flowing Ar-N<sub>2</sub> microwave discharge*, J.Phys.D **24**, 909-914
31. J.Wang, S.T.Sanders, J.B.Jeffries, and R.K.Hanson, 2001, *Oxygen measurements at high pressures with vertical cavity surface-emitting lasers*, Appl.Phys.B **72**, 865-872
32. P.Vogel, and V.Ebert, 2001, *Near shot noise detection of oxygen in the A-band with vertical-cavity surface-emitting lasers*, Appl.Phys.B **72**,127-1353
33. A.V.Timofeev,1997, *Theory of microwave discharges at atmospheric pressures*, Plasma Physics Reports, Vol. 23, 158-164